# On-the-go assessment of vineyard canopy porosity, bunch and leaf exposure by image analysis

M.P. DIAGO[1,2], A. AQUINO[3], B. MILLAN[3], F. PALACIOS[1,2] and J. TARDAGUILA[1,2]

[1] Department of Agriculture and Food Science, University of La Rioja, Logroño 26006, Spain; [2] Instituto de Ciencias de la Vid y del Vino, University of La Rioja, Consejo Superior de Investigaciones Científicas, Logroño 26007, Spain; [3] Department of Electronic Engineering, Computer Systems and Automation, University of Huelva, Huelva 21819, Spain
Corresponding author: Professor Javier Tardaguila, email javier.tardaguila@unirioja.es

## Abstract

**Background and Aims:** Canopy assessment of the fruiting zone can lead to more informed vineyard management decisions. A non-destructive, image-based system capable of operating on-the-go was developed to assess canopy porosity, and leaf and bunch exposure of red grape cultivars in the vineyard.

**Methods and Results:** On-the-go (7 km/h) night time images of a vertically shoot positioned commercial vineyard canopy were acquired with an automated red green blue imaging system, coupled to a GPS and controlled artificial lighting. The reference method was point quadrat analysis. Sound correlations between the image analysis and point quadrat analysis results for the proportion of gaps ($R^2 > 0.85$; $P < 0.001$) and leaf to canopy area ratio ($R^2 > 0.57$; $P < 0.001$) were obtained for both sides of the canopy. For the bunch to canopy area ratio the best relationship was found on the western side of the canopy ($R^2 = 0.79$; $P < 0.001$). Also maps of the three canopy variables were built in a commercial vineyard to compare their spatial variability on the east and west sides across the whole vineyard plot.

**Conclusions:** The developed imaging system, capable of operating on-the-go, can yield quantitative, objective and reliable knowledge of what a grapegrower would assess by subjective, qualitative visual inspection of the grapevine canopy. The information can be used to help make better informed decisions about leaf removal, and if mapped may help to delineate zones amenable to homogeneous management.

**Significance of the Study:** The new developed computer vision system can be mounted on any vehicle, such as a tractor, all terrain vehicle and robot, for a rapid and objective monitoring of the vineyard canopy around the fruiting zone in red cultivars and vertically shoot positioned trained vines. Moreover, the maps generated could be used by a new generation of variable rate viticultural machinery to spatially optimise vineyard cultural practices.

***Keywords:*** *canopy gap, computer vision, defoliation, grapevine, point quadrat analysis, precision viticulture*

## Introduction

In viticulture, canopy features, such as leaf area, canopy porosity and fruit exposure, are key factors that can be manipulated through canopy management to manage yield and fruit composition (Smart 1992). Canopy management practices leading to improved leaf and bunch exposure have been shown to result in better yield and wine quality (Smart and Robinson 1991, Main and Morris 2004, Kliewer and Dokoozlian 2005). The amount of exposed leaf area in the canopy is an important factor, as each layer of leaves captures around 94% of the incident photosynthetically active radiation (Smart 1987, Smart and Robinson 1991). Canopy gaps are beneficial to fruit as airflow reduces the chance of crop losses due to fungal disease (Austin et al. 2011). Therefore, in terms of ideal grapevine canopy porosity, values range from 10 to 20% according to Palliotti and Silvestroni (2004) or between 20 and 40% gaps, as suggested by Smart (1987) in his scorecard for assessing potential winegrape quality, to ensure optimum sunlight interception. Bunch exposure needs to be balanced. On one hand, sun exposure favours synthesis of aroma/flavour compounds (Reynolds and Wardle 1989, Diago et al. 2010) as well as other secondary metabolites, such as flavonols and anthocyanin pigments in fruit (Tardaguila et al. 2012, Diago et al. 2012a). Excessive fruit exposure, however, mainly in warm growing regions, can also lead to sunburnt berries and a loss of grape anthocyanins, hence berry colour (Kliewer 1977, Mori et al. 2007). In order to improve canopy management, by focusing on ensuring a proper distribution of leaves and gaps around bunches (Smart 1992), a method is needed to quantify the main canopy characteristics in the fruiting zone that is objective, rapid and automated.

New and non-invasive sensing technologies can be applied to assess vineyard canopy. Computer vision is a non-invasive technology, which involves the automated acquisition, analysis and understanding of useful information from a single image or a sequence of images. In viticulture, the use of computer vision outdoors from still photography with visible [red green blue (RGB)] cameras has been used to characterise different features of the vineyard (Tardaguila et al. 2010, Hill et al. 2011) and to estimate yield components (Dunn and Martin 2004, Nuske et al. 2014, Liu et al. 2017). Recent work has advanced our ability to assess canopy features from RGB imaging in grapevines (Diago et al. 2012b, 2016) and in other crops (Chopin et al. 2016, 2018) by adopting colour corrections and hybrid approaches of the classification algorithms. With the exception of the work of Nuske et al. (2014) and Liu et al. (2017), studies have involved static, point-to-point, manual image

doi: 10.1111/ajgw.12404

acquisition, which from a practical standpoint, is a constraint when a large number of grapevines need to be assessed. Thus, there are still some practical limitations to the adoption of RGB imaging as a commercial monitoring method, such as the manual and static mode of image acquisition or the use of a colour background.

The necessary steps towards automation and on-the-go canopy assessment using computer vision were outlined by Gatti et al. (2016), who installed a system equipped with matrix-based optical RGB sensors on a conventional tractor to assess, on a stop and go mode, the leaf layer number and fractions of canopy gaps and interior leaves during day time. Other authors have used RGB imagery acquired at night time from an autonomous moving platform, at low speed (0.3 km/h) to reconstruct a textured three-dimensional (3D) point cloud to quantify yield components (Rose et al. 2016). While the merit of these initiatives is valuable, the implementation of precision viticulture and variable rate machinery demands a non-invasive system capable of assessing the main canopy features on-the-go, at a speed that is commercially acceptable (3–7 km/h) (Martin-Clouaire et al. 2016).

Fully on-the-go approaches at a speed close to commercial values have been achieved by several authors using different sensing technologies, such as laser scanning (Llorens et al. 2010, Gil et al. 2013) and ultrasound (Palleja and Landers 2017) to determine canopy density in grapevines and in olive trees or to estimate the pruning mass in vineyards (Tagarakis et al. 2013). Having reliable information, however, on several canopy elements (gaps, leaves and bunches) around the fruiting zone simultaneously would be of value. Therefore, the goal of this study was to develop a new, objective, non-invasive imaging system to assess the key bunch zone parameters of grapevine canopies, viz. exposed fruit and leaf area and the proportion of gaps using images acquired on-the-go and at commercial speed.

## Materials and methods

### *Vineyard site and experimental layout*

The trials were conducted in season 2015 in a commercial Tempranillo (clone ISV-F-V6 planted on rootstock SO4) vineyard located in Ábalos (latitude 42°34′44.1″N; longitude 2°42′24.0″W; La Rioja, Spain), denoted as vineyard site #1. The vines were planted in north–south orientation in 2006, dry-grown, spur-pruned on a bilateral cordon to retain eight spurs and two buds per spur and trained onto a vertical shoot positioned (VSP) trellis system with 2.5 m row spacing and 0.8 m vine spacing. All plants were defoliated on the east side after berry set (*E*-L stage 32) (Coombe 1995) as this is a common practice in the Rioja Wine Appellation to promote better airflow and bunch exposure.

For data acquisition, 50 consecutive canopy vineyard segments comprising three adjacent vines each (150 vines in total) were labelled. For each segment, the three canopy parameters, canopy porosity or gaps to canopy area ratio (%), exposed leaves to canopy area ratio (%) and exposed bunches to canopy area ratio (%), were estimated using image analysis (details described below) and benchmarked against reference point quadrat analysis (PQA) measurements (Smart and Robinson 1991).

Once the image-analysis methodology was developed, it was used to assess the spatial variability of the canopy features of another commercial vineyard plot, denoted as vineyard site #2. Vineyard site #2 was located in Logroño (latitude 42°28′32.3″N; longitude 2°28′58.8″W, 630 masl; La Rioja, Spain). Site #2 was a plot of 4.0 ha of Tempranillo, spur-pruned on a bilateral cordon to retain eight spurs and two buds per spur and trained onto a VSP trellis system with 2.5 m row spacing and 0.8 m vine spacing. Vines were planted in year 2006, with rows oriented north–south. All plants were defoliated on its east side at bunch closure (*E*-L stage 32) (Coombe 1995).

### *In-field measurements*

**Image acquisition.** The images of the vineyard canopy were acquired and processed in real time using a human-driven multi-sensor platform (Televitis mobile laboratory) developed at the University of La Rioja, Logroño, Spain. This mobile sensing platform incorporated the following elements (Figure 1):

- *All-terrain vehicle (ATV)*: a Trail Boss 330 (Polaris Industries, Medina, MN, USA) was used (Figure 1a).
- *RGB camera*: a Sony α7II RGB camera (Sony, Tokyo, Japan) equipped with a Zeiss 24/70 mm lens (Zeiss, Oberkochen, Germany) with optical stabilisation was selected for the purposes of this study. This is a mirrorless camera mounting a full-frame complementary metal oxide semiconductor sensor (35 mm, and 24.3 megapixel resolution), which provides high light sensitivity and low noise generation. Furthermore, the camera also incorporates a five-axis sensor stabilisation system and offers high shutter speed and quick image storage (Figure 1b).
- *Artificial illumination system*: a white-light emitting diode panel was incorporated into the platform (Figure 1c) to enable the vines to be imaged during the night.
- *Sensor supporting structure*: a modular and adaptable structure was designed and built with commercial aluminium profiles. The structure consisted of two fixed trays, one upfront and one on the rear part, and an adjustable arm to be installed in the front tray (Figure 1a). The arm was used to mount the RGB camera and illumination system and to make the combination adjustable to variable vineyard height (Figure 1b).
- *GPS receiver*: a Leica Zeno 10 Global Positioning System (Heerbrug, St Gallen, Switzerland) was used to georeference the images (Figure 1d) with real-time kinematic correction, working at <30 cm precision.
- *Inductive sensor for camera triggering*: an inductive sensor was installed in the rear axle. This sensor produced three activation pulses per wheel-spin for triggering the camera (Figure 1e).
- *Custom-built electronic control system*: an electronic control system based on the Arduino MEGA development board (Arduino, Ivrea, Italy) was built to integrate hardware and to trigger the camera using a galvanically isolated signal (Figure 1d). The system also allows for data storage (GPS position to image association) in an secure digital card and for showing capture-status information in a 12.45 cm thin film transistor screen.

The mobile sensing platform allowed the capture, and storage on-the-go, of three images per wheel-spin at around 7 km/h, producing high-quality images despite the vibrations caused by the ATV engine and the irregular ground surface. Images were acquired at night time using the artificial illumination system from the multi-sensor moving platform (Figure 2a). Under natural sunlight conditions, the whole scene was equally illuminated, producing images in

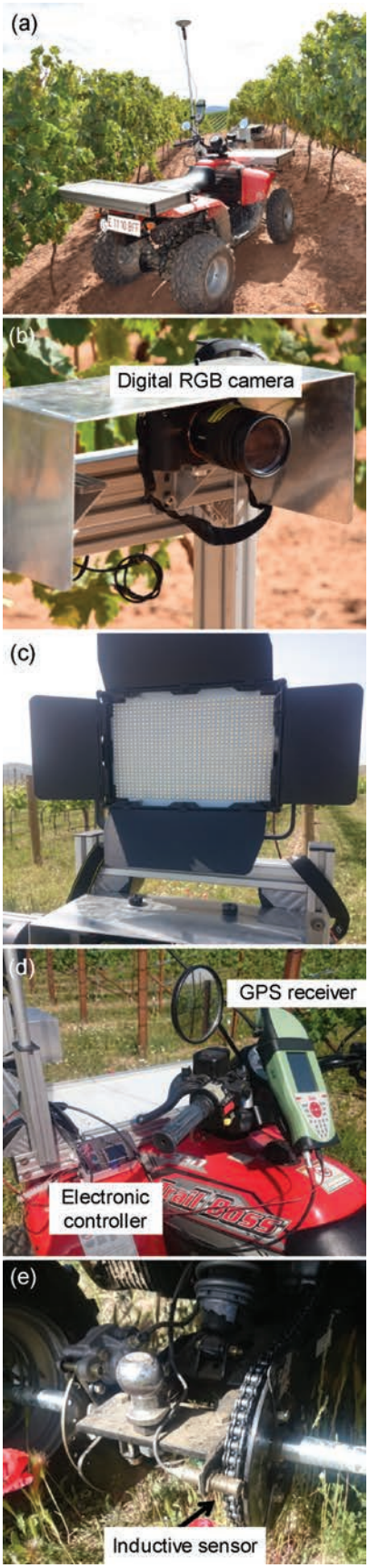


**Figure 1.** Illustration of the multi-sensor mobile platform developed for the on-the-go image acquisition in the vineyard: (a) general view of the multi-sensor mobile platform; (b) red green blue (RGB) camera installed in the platform by means of an ad hoc designed structure; (c) light emitting diode illumination panel; (d) detail of the custom-built electronic control system and GPS receiver; and (e) inductive sensor installed in the rear axle for automatically triggering the camera.

which the vines under study were hardly distinguishable from those in opposite rows. In the present work, the isolation (in the image) of the vines under evaluation from those in the opposite row was successfully achieved by means of illumination and camera parameterisation (Figure 2b). The arm was adjusted for the camera to be at around 1.5 m away from the canopy. The camera was set in manual mode, configuring the aperture in f/4, shutter speed in 1/2500 s, ISO sensitivity in 5000 and focus in manual mode.

**Point quadrat analysis reference measurements.** Point quadrat analysis was undertaken on the same day as the photographs were acquired, after Smart and Robinson (1991) on the first 50 cm above the cordon (fruiting zone). A 5 mm diameter stainless steel probe was used for PQA insertions. For each segment of three adjacent vines, 50 insertions through the canopy at approximately 15 cm horizontal intervals at a height of 10, 30 and 50 cm above the cane were made. For each insertion, the sequential contacts with the vineyard canopy elements from one side of the canopy to the other were recorded using L (leaf) or B (bunch). In the case of no contact with vine elements during the insertion, G (gap) was registered.

Two different approaches were used to compute the proportion of external or exposed leaves and exposed bunches from the PQA insertions. The first approach aimed to mimic the two-dimensional image analysis. In this case, the proportion (%) of exposed leaves or bunches was computed separately for each canopy side (east and west) as the ratio between the number of first L or B contacts, divided by the total number of insertions, multiplied by 100. Two indices, respectively, were calculated for the east and west sides, of the proportion of exposed leaves$_{side}$ (%) using Equation 1.

$$\text{Proportion of exposed leaves}_{side}(\%) = \frac{\#\text{L (only first contacts)}}{\#\text{ Insertions}} \times 100 \quad (1)$$

Similarly, two indices, proportion of exposed bunches$_{east}$ (%) and proportion of exposed bunches$_{west}$ (%) were calculated with Equation 2.

$$\text{Amount of exposed bunches}_{side}(\%) = \frac{\#\text{B (only first contacts)}}{\#\text{ Insertions}} \times 100 \quad (2)$$

The second approach intended to estimate the proportion of exposed leaves or bunches of the whole vine segment, and for this reason both sides of the canopy were assessed. For this second approach the proportion of exposed leaves or bunches was calculated as the ratio of all external (first or last contacts) L or B, divided by the total number of insertions multiplied by 2, respectively, then multiplied by 100 (Equations 3, 4).

$$\text{Proportion of exposed leaves}_{vine}(\%) = \frac{\#\text{L (first or last contacts)}}{\#\text{ Insertions} \times 2} \times 100 \quad (3)$$

$$\text{Proportion of exposed bunches}_{vine}(\%) = \frac{\#\text{B (first or last contacts)}}{\#\text{ Insertions} \times 2} \times 100 \quad (4)$$

The canopy porosity or proportion of gaps in the fruiting zone was calculated as the total number of gaps G divided


**Figure 2.** (a) On-the-go image acquisition with the multi-sensor mobile platform; and (b) image acquired with artificial illumination in which, due to appropriate illumination and camera parametrisation, the vines under evaluation are discernible from the darkened background.

by the number of insertions, multiplied by 100, as described in Equation 5.

$$\text{Canopy porosity}\,(\%) = \frac{\#\text{G}}{\#\ \text{Insertions}} \times 100 \qquad (5)$$

### *Image processing and analysis*

**Image processing.** Three images per wheel-spin were acquired on-the-go with the multi-sensor moving platform. This frequency, along with the circumference of the wheel in the sensor-equipped ATV and the distance of the camera to the canopy, ensured that vines of interest were always imaged. This also produced redundant information in images, however, since two consecutive images always contained a repeated vine section (Figure 3a–c). To avoid the analysis of redundant data, images were matched using the Auto Blend tool provided by Adobe Photoshop CC 2015 (Adobe Systems, San Jose, CA, USA) to this effect. Thus, mosaic images were created, which were then analysed piecewise (hereafter, these pieces will be generically called images for simplification) using a pixel-classification approach (Figure 3d).

The pixel classifier was an improved version of the one based on the Mahalanobis distance (Mahalanobis 1936) presented by Diago et al. (2012b). The classifier was trained using supervised learning. For that, first, the following five sets covering the expected objects in the images were defined: 'bunch', 'trunk', 'shoot', 'leaf', 'gap' and 'trellis'. Then, the classifier was trained by manually selecting 500 pixel samples per set (3000 training instances in total), carefully covering as much variability as possible for every set. Mathematically, a pixel $p_i$ was defined by the following six-dimensional vector:

$$p_i = (R_i, G_i, B_i, H_i, S_i, V_i)$$

$R_i$, $G_i$ and $B_i$ correspond to the pixel's red, green and blue values according to the RGB colour space, respectively. Furthermore, $H_i$, $S_i$ and $V_i$ stand for the pixel's hue, saturation and value in the hue saturation value (HSV) colour space, obtained by means of space conversion (Agoston 2005). These last three values from the HSV colour space were not included in the original version of the classification algorithm (Diago et al. 2012b), so they were incorporated in this study. In addition to this mathematical 'double-colour space' approach, two additional classifiers including information from only one of them were also implemented for comparison purposes. Thus, the pixel vectors for the RGB classifier were defined as

$$p'_i = (R_i, G_i, B_i)$$

and

$$p''_i = (H_i, S_i, V_i)$$

for the HSV version. The performance of all three classifiers was tested and compared.

For the three classifiers individually, once they were trained, images were analysed to obtain classification outcomes. This is, for a given image under analysis, every pixel was classified as 'bunch', 'trunk', 'shoot', 'leaf', 'gap' or 'trellis" (posts + wires). Figure 4a shows an example image and Figure 4b the resulting image produced by the classification algorithm implementing the 'double-colour space' approach. The last step consisted on improving the classification yielded by the algorithm by correcting misclassified pixels, as described below.

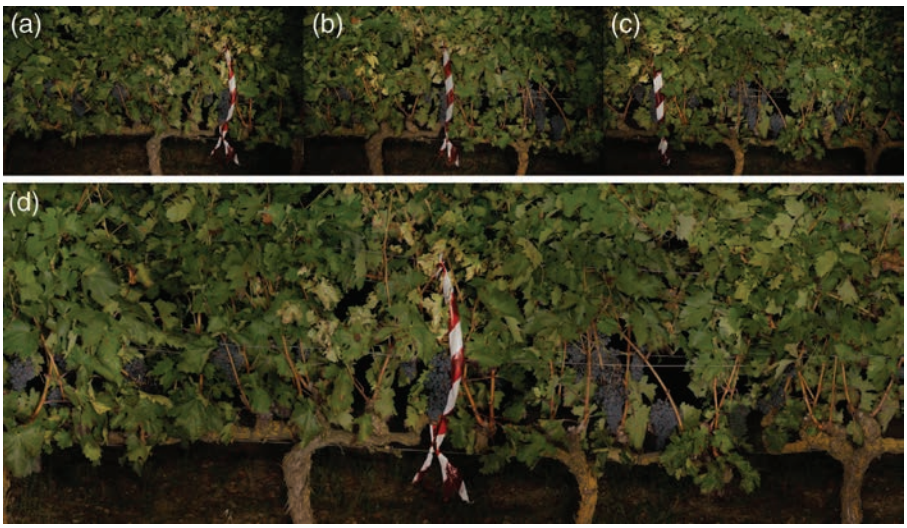


**Figure 3.** Image pre-processing illustration: (a), (b) and (c) show images automatically acquired during a wheel-spin with the multi-sensor mobile platform. To identify overlapping areas between the images, note that the red and white tape in them was exactly the same; (d) resulting images after matching images (a), (b) and (c).

For the classified image shown in Figure 4b, the majority of misclassifications referred to the 'bunch' class. On the one hand, there were many isolated 'bunch' pixels within canopy gaps. This was caused by the fact that in parts of the bunches with shadows, the dark-red colour of grapes was much darker (almost black) in the images. In contrast, some portions of bunches were filled with 'leaf' pixels. This was due to the epicuticular wax of berries tending to yield greenish tones. These two general classification mistakes were corrected by post-processing classified images using mathematical morphology, specifically the erosion and dilation operations (Soille 2004). In the classified images (Figure 4b), isolated 'bunch' pixels were removed as a first step by applying a morphological erosion (Soille 2004) on this set using a small disc as structuring element (SE). With this operation, all 'bunch' particles smaller than the SE were removed. Additionally, all remaining 'bunch' objects in the eroded images were diminished according to the size of the SE. To recover the original size and shape of these objects, a morphological reconstruction (Soille 2004) by dilation on the 'bunch' set of classified images was performed.

The last step involved the filling of the gaps or holes within bunches employing the morphological fill-hole operator (Soille 2004). The results of the application of the image processing described here are presented in Figure 4c.

**Image derived canopy parameters.** For the computation of the canopy parameters a double approach to delimitate the region of interest (ROI) was followed. In vineyard site #1 in order to guarantee that image-analysis outcomes were compared to PQA reference measurements rigorously over the same canopy area, images were manually cropped to match the fruiting zone, that is, the first 50 cm above the vine cordons. Likewise, all classified images were manually cut to match the ROI comprising the first 50 cm above the vine cordons (fruiting zone) defined during PQA measurements. In vineyard site #2, an automated procedure was developed for setting a ROI in every image. It consisted on, given a segmented image, finding an upper and a lower cut point to delimit a ROI corresponding to the fruiting zone. These cut points are the central points on the vertical axis of two rectangular regions of a fixed size which have a proportion of pixels not assigned to 'leaf' class (for the upper cut) and not assigned to 'leaf' or 'bunch' class (for the lower cut) below a certain threshold. The regions are determined by searching iteratively across the image on the vertical axis. Once the ROIs were delimited in both vineyard sites, the following indices obtained by image analysis were computed:

- *Fruiting zone canopy porosity or gaps to canopy area ratio (%)*: it was calculated as the number of 'gap' pixels divided by the total number of pixels in the ROI, multiplied by 100 (Equation 6).

$$\text{Canopy porosity to canopy area ratio}_{\text{vine}}(\%) = \frac{(\#\text{Gap pixels})}{(\#\text{ROI pixels})} \times 100 \quad (6)$$

- *Bunches to canopy area ratio (%)*: it was calculated separately for each canopy side (east and west) as the number of 'bunch' pixels divided by the total number of pixels in the ROI, multiplied by 100. For the computation of the proportion of exposed bunches (%) of the whole vine segment, Equation 7 was used:

$$\text{Bunches to canopy area ratio}_{\text{vine}}(\%) = \frac{(\#\text{Bunch pixels}_{\text{east}} + \#\text{Bunch pixels}_{\text{west}})}{(\#\text{ROI pixels}_{\text{east}} + \#\text{ROI pixels}_{\text{west}})} \times 100 \quad (7)$$

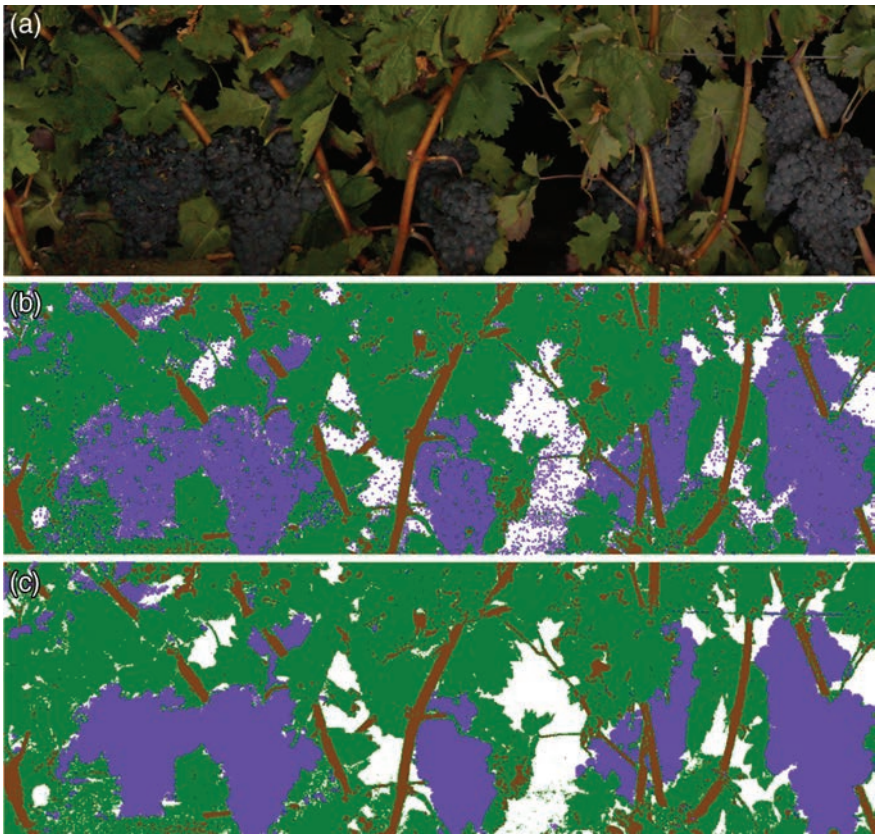


**Figure 4.** Result of the image processing and analysis: (a) close-up of a vine image; (b) result of the analysis of image (a) in which pixels are represented in the colour associated to their assigned class; and (c) result of post-processing image (b) in which holes within bunches are filled and isolated bunch pixels are removed.

- *Exposed leaves to canopy area ratio (%)*: it was calculated separately for each canopy side (east and west) as the number of 'leaf' pixels divided by the total number of pixels in the ROI image, multiplied by 100. For the computation of the proportion of exposed leaves (%) of the whole vine segment (similar to total exposed leaf area per vine segment without taking into account the zenithal top part of foliage), Equation 8 was used:

$$\text{Exposed leaves to canopy area ratio}_{\text{vine}}(\%) = \frac{(\#\text{Leaf pixels}_{\text{east}} + \#\text{Leaf pixels}_{\text{west}})}{(\#\text{ROI pixels}_{\text{east}} + \#\text{ROI pixels}_{\text{west}})} \times 100 \quad (8)$$

**Mahalanobis-based classifier evaluation.** The defined classification cases (Kohavi and Provost 1998) were computed from classifier's predictions on each test set of a tenfold stratified cross validation performed on the 3000 pixel training instances to compare the predictive capability of the RGB–HSV colour combined model against that of the RGB and HSV separate models. For each class, a binary case was considered (e.g. bunch class against not-bunch classes) and four main values were obtained:

- *True positives (TP)*: number of pixels belonging to the class under evaluation, correctly classified as instance from that class;
- *False positives (FP)*: number of pixels not belonging to the class under evaluation, incorrectly classified as instance of that class;
- *True negatives (TN)*: number of pixels not belonging to the class under evaluation, correctly classified as instance from any other class; and
- *False negatives (FN)*: number of pixels belonging to the class under evaluation, incorrectly classified as instance from any other class.

The sensitivity (Equation 9), specificity (Equation 10) and precision (Equation 11) classification performance metrics were calculated from these values for the three models:

$$\text{Sensitivity} = \frac{\text{TP}}{\text{TP} + \text{FN}} \quad (9)$$

$$\text{Specificity} = \frac{\text{TN}}{\text{TN} + \text{FP}} \quad (10)$$

$$\text{Precision} = \frac{\text{TP}}{\text{TP} + \text{FP}} \quad (11)$$

In addition, the F1 score and the Matthews correlation coefficient (MCC) were also computed (Equation 12). The F1 score is defined as the harmonic mean of Precision and Sensitivity (also known as Recall) (Chinchor 1992) (Equation 12):

$$F_1 = 2 \times \frac{\text{Precision} \times \text{Sensitivity}}{\text{Precision} + \text{Sensitivity}} \quad (12)$$

The F1 score reflects the accuracy of the classification, as it combines the Sensitivity and Precision indicators.

The MCC is a performance metric which provides information on the accuracy of the quality of a binary (two-class) classification (Matthews 1975) and it is considered to perform better than Sensitivity and Specificity in binary classifications (Powers 2011) (Equation 13).

$$\text{MCC} = \frac{\text{TP} \times \text{TN} - \text{FP} \times \text{FN}}{\sqrt{(\text{TP} + \text{FN}) \times (\text{TP} + \text{FP}) \times (\text{TN} + \text{FP}) \times (\text{TN} + \text{FN})}} \quad (13)$$

### *Statistical analysis*

Linear regression analysis was performed for each canopy parameter of interest on data obtained from image analysis and the PQA method, and the determination coefficients ($R^2$) were computed. All calculations and plots were carried out using Sigma Plot 12.0 (Systat Software, San Jose, CA, USA).

### *Mapping*

The developed computer vision system was applied in vineyard site #2 for mapping canopy porosity, leaf and bunch exposure. Every other row was monitored, half of them on the west side and the other half on the east side of the canopy with the same multi-sensor mobile platform at 7 km/h. All the image acquisition parameters and set up were the same as described earlier in this study. Images acquired on-the-go were analysed using the developed classification algorithm which yielded the best performance indicators. From this analysis, a set of georeferenced measurements of the three parameters was obtained. This set was mapped using ordinary kriging with ArcGIS 10.4 (ESRI, Redlands, CA, USA), and three statistical clusters for each canopy feature were defined and represented using the Jenks natural breaks optimisation method (Jenks 1967).

## Results

### *Comparison of the classifiers' performance*

The processing of images to identify the bunches, leaves, shoots and trellis was done on a pixel-by-pixel basis, resulting in a dense map where each pixel in the image was assigned to a class. This approach required post-processing to remove outlier pixels that did not match the class of their surrounding pixels. The solution proposed, however, was selected to obtain an optimum balance between computational cost (methodological complexity) and accuracy. Certainly, more complex and heavier solutions based on the design and calculation of texture descriptors along with more complex classifiers, such as support vector machine or neural networks (Herrera et al. 2016), could be explored with satisfying results as well. Nevertheless, for the sake of real-time high-resolution image processing, the presented methodology, based on a compact classifier followed by some steps of mathematical morphology for post-processing was chosen, thus obtaining a simpler but accurate alternative for semantic classification of pixels.

While the three classification approaches (RGB, HSV and RGB + HSV) yielded similar results for the three main classes under consideration (gap, leaf and bunch) in terms of sensitivity and specificity, the 'double-colour space' approach (RGB + HSV) and the individual HSV classification model proved to be slightly superior to the RGB model according to the F1 score and the MCC values (Table 1). Even less differences existed between RGB + HSV and HSV, but the 'double-colour space' classifier performed equally well or better than the HSV classifier for the bunch class for the four performance indicators evaluated (Table 1). For this reason, all subsequent image-analysis

results and comparison against the PQA measurements were obtained from image classification processes using the 'double-colour space' classifier. These results agree with other studies, in which the simultaneous use of information from different colour spaces to create a hybrid colour space (Vandenbroucke et al. 1998, Maktabdar Oghaz et al. 2015) or, as in this work, the combined use of two-colour spaces has proved to yield satisfactory results in human skin detection and classification (Subban and Mishra 2013).

### *Assessment of grapevine canopy features*

A wide range of canopy porosity (expressed as proportion of gaps in the fruiting zone) which spanned from approximately 10–50% (Figure 5) was sampled in the vineyard and used for the calibration between the image-derived canopy variables and those measured by PQA (vineyard site #1). For this, strong correlations, with $R^2$ above 0.85 ($P < 0.001$), were obtained for both sides of the canopy (Figure 5a,b) and the two-side average (Figure 5c). Similarly, the correlation between the proportion of gaps determined by image analysis from the east and west sides of the canopy ($y = 1.031x - 2.832$) yielded a $R^2 = 0.95$ ($P < 0.001$), being the value of the slope significantly equal to 1 ($P = 0.445$) (Figure 6).

The best correlation for the comparison between the amount of exposed bunches as determined by PQA and the bunch to canopy area ratio (%) from image analysis (Figure 7), was achieved on the west side, with $R^2 = 0.61$ ($P < 0.001$) (Figure 7b). Relationships corresponding to the east side of the canopy ($R^2 = 0.32$; $P < 0.001$) (Figure 7b) and to a whole vine basis ($R^2 = 0.37$; $P < 0.001$) (Figure 7c) showed lower $R^2$ values.

The correlations between the image analysis and PQA data (Figure 8a–c) for the leaf class yielded $R^2$ values close to or above 0.60 in all cases ($P < 0.001$), while the strongest relationship was also obtained from data acquired on the west side ($R^2 = 0.79$, $P < 0.001$) (Figure 8a).

While for the canopy porosity (Figure 5) and the canopy leaf information (Figure 8), the range of the scale of the two correlated variables was comparable, for the bunch class, the range for the PQA measurements (from 0 to 50%) and for the image analysis (between 0 and 15%) were substantially different.

**Table 1.** Sensitivity results, specificity, F1 score and Matthews correlation coefficient of the pixel classification methodology in several canopy classes on the training set using a tenfold stratified cross validation for the individual use of red green blue (RGB), hue saturation value (HSV) and jointly both RGB and HSV colour spaces.

| Vineyard canopy class | RGB + HSV† | RGB | HSV |
|---|---|---|---|
| **Sensitivity** | | | |
| Trellis | 0.862 | 0.846 | 0.842 |
| Gap | 0.960 | 0.918 | 0.970 |
| Leaf | 0.934 | 0.954 | 0.940 |
| Shoot | 0.858 | 0.900 | 0.818 |
| Trunk | 0.856 | 0.856 | 0.880 |
| Bunch | 0.938 | 0.874 | 0.938 |
| **Specificity** | | | |
| Trellis | 0.982 | 0.984 | 0.982 |
| Gap | 0.995 | 0.997 | 0.993 |
| Leaf | 0.991 | 0.985 | 0.992 |
| Shoot | 0.980 | 0.976 | 0.987 |
| Trunk | 0.953 | 0.940 | 0.951 |
| Bunch | 0.981 | 0.986 | 0.972 |
| **F1 Score** | | | |
| Trellis | 0.883 | 0.879 | 0.871 |
| Gap | 0.967 | 0.950 | 0.967 |
| Leaf | 0.943 | 0.944 | 0.950 |
| Shoot | 0.876 | 0.890 | 0.869 |
| Trunk | 0.818 | 0.794 | 0.829 |
| Bunch | 0.924 | 0.900 | 0.904 |
| **Matthews correlation coefficient** | | | |
| Trellis | 0.861 | 0.856 | 0.847 |
| Gap | 0.960 | 0.942 | 0.961 |
| Leaf | 0.932 | 0.932 | 0.941 |
| Shoot | 0.851 | 0.868 | 0.847 |
| Trunk | 0.781 | 0.752 | 0.794 |
| Bunch | 0.909 | 0.881 | 0.884 |

†Colour space.

### *Mapping*

Maps of the spatial variability of the three main elements of the canopy, gaps, leaves and bunches, for the commercial vineyard (site #2) assessed by on-the-go imaging are presented in Figure 9. Since the canopy porosity of the fruiting zone assessed from east and west sides was found to be the same (Figure 6), a unique map involving the rows imaged on the two sides was built (Figure 9a). As observed in Figure 9a, most of the vineyard (76.2% of the surface) exhibited a canopy porosity ranging from ~40 to 50% gaps. In terms of the bunch to canopy area ratio (%) (Figure 9b,c) and leaves (Figure 9d,e), the differences between east and west maps were mostly quantitative, as similar variability patterns were found between the two sides. In the case of the exposed leaves, slightly lower values (from ~26 to 50%) were observed in the map corresponding to the east side (defoliated) (Figure 9d), as compared to that of the west side (Figure 9e). In both sides, the lowest values were found at the north-west edge of the plot, while an area with larger values of leaf to canopy area ratio (%) was identified in the south-east and the centre of the east boundary of the vineyard. The pattern of bunch exposure revealed increased values on the west boundary of the vineyard, which tended to lessen towards the east direction of the plot, although the values of the bunch to canopy area ratio were low and similar across the whole plot.

## Discussion

The results obtained in the present work demonstrate the capability of the developed RGB image-based system, operated on-the-go at commercial speed, to successfully determine the canopy porosity in the fruiting zone and to provide useful information about the leaf and bunch to canopy area ratios at the fruiting zone on red cultivars trained to a VSP trellis. The on-the-go imaging system can provide a quantitative, objective and reliable measure of what a grapegrower would assess by subjective, qualitative visual inspection of the grapevine canopy. Among the different methods for canopy assessment, Smart (1992) reported the PQA, sunfleck measurement or visual scoring using a scoresheet (Smart and Robinson 1991). Although the first two methods provide quantifiable data, they are time and labour consuming. Therefore, canopy assessment is mostly based on purely visual inspection. These visually gathered inputs are often used by the viticulturist to assist with making canopy management decisions about defoliation. In addition to single-wire VSP grapevines, the developed image-based methodology could be applied to other vertical trellis systems, such as Scott Henry or Smart-Dyson.

Using the developed image-analysis system, the information about the main elements of the canopy at the fruiting

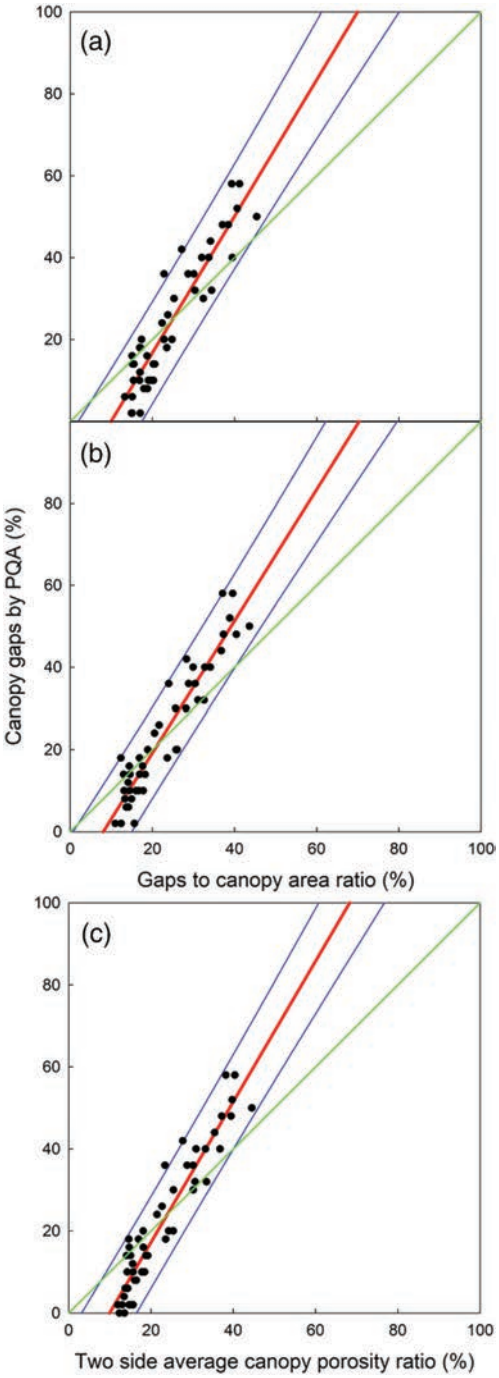


**Figure 5.** Correlations between the proportion of gaps or canopy porosity, assessed by analysis of images acquired using the multi-sensor platform on-the-go and the reference values determined by point quadrat analysis (PQA), from (a) the east side of the canopy ($R^2$ = 0.86); (b) the west side of the canopy ($R^2$ = 0.89); and (c) the whole vine, showing the average value from east and west sides of the canopy ($R^2$ = 0.90). All determination coefficients ($R^2$) were significant at $P < 0.001$. Correlation line (——), prediction bands at 95% (——), the 1:1 line (——) ($n$ = 50).

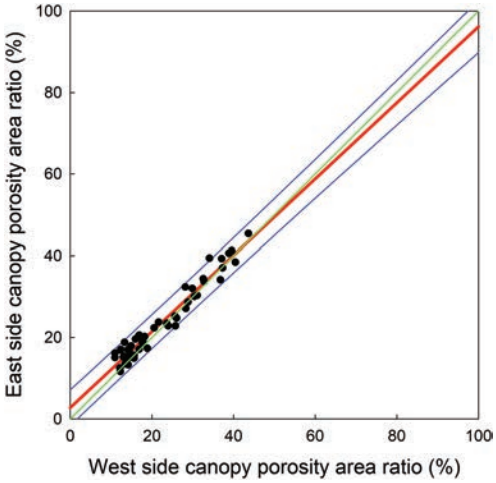


**Figure 6.** Correlation between the proportion of gaps or canopy porosity, assessed by image analysis from images acquired on east and west sides of the canopy, using the multi-sensor platform on-the-go. Coefficient of determination $R^2$ = 0.95, at $P < 0.001$. Correlation line (——), prediction bands at 95% (——), the 1:1 line (——) ($n$ = 50).

zone can be obtained separately from the two sides of the canopy or integrated in a single value. This constitutes different, but complementary, information to that gathered by aerial remote sensing solutions. Remote sensing from different airborne platforms (remotely piloted aircraft or manned aircraft) is commercially available in most viticultural regions worldwide. In commercial remote sensing operations, spectral information (as well as thermal information) about canopy vegetation (mostly from above the vines) is provided, usually expressed as spectral indices, such as the normalised difference vegetation index (NDVI) or plant cell density (PCD), depending on the band configuration of the multi-spectral or hyperspectral camera. These spectral data provide information about vine vigour, biomass and overall greenness of the canopy, but do not specifically provide information about leaf, gap and bunch distribution and configuration in the fruiting zone. Such viticultural parameters have an impact on bunch microclimate, air circulation and bunch exposure, which in turn affect disease risk and fruit ripening and fruit composition, and botrytis incidence as described by Smart (1992). The spectral information obtained from remote sensing can be used to delineate homogeneous vigour areas and potentially define differential harvesting schedules according to this zonal delineation. However, whether increase of bunch exposure is required or not, leading to decisions about leaf removal cannot be inferred only from remote sensing monitoring. While it could be assumed that the spatial structure of NDVI or PCD (remotely assessed) would not differ markedly from the spatial structure of canopy gaps, especially when classified into a low and limited number of classes (e.g. low, medium and high), the need for ground-truthing is essential. Recent studies have postulated the importance of providing detailed ground-truthing of remotely sensed NDVI-based vigour maps (Gatti et al. 2017). These authors stated that overall assessment of vine performance by NDVI may help to classify the vineyard areas according to their vigour, but this attribution can be 'misleading' if no site-specific ground-truthing is conducted. In this context, the developed RGB methodology may also help in to facilitate ground-truthing at a large scale.

Moreover, the capability of separately monitoring the two canopy sides is of special relevance when canopy management operations, such as leaf removal, are performed only on one side. This is a common practice in many wine regions, where grapegrowers defoliate the morning side to improve fruit exposure and airflow during the cooler hours of the day during the ripening period (Dokoozlian 2009). With the developed computer vision system, a picture of the leaf distribution, porosity and bunch exposure in the fruiting zone of vertically trellised vineyards, and the required adjustments required in each side can be envisaged.

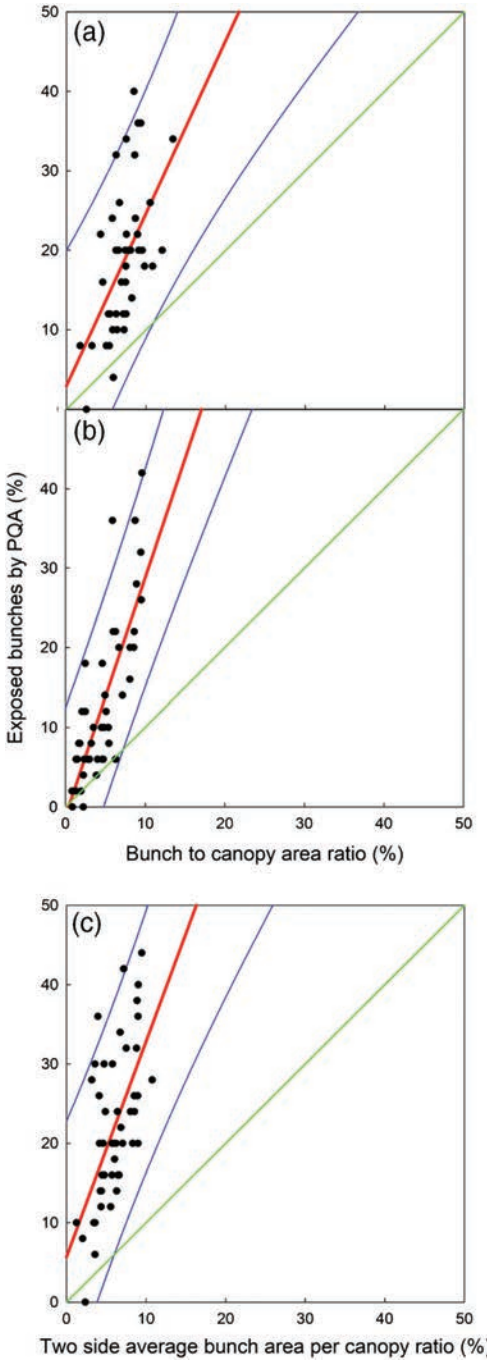


**Figure 7.** Correlations between the bunch to canopy area ratio (%) assessed by image analysis from images acquired using the multi-sensor platform on-the-go and the values determined by point quadrat analysis (PQA), from (a) the east side of the canopy ($R^2$ = 0.32); (b) the west side of the canopy ($R^2$ = 0.61); and (c) the whole vine ($R^2$ = 0.37). All determination coefficients ($R^2$) were significant at $P < 0.001$. Correlation line (——), prediction bands at 95% (——), the 1:1 line (——) ($n$ = 50).

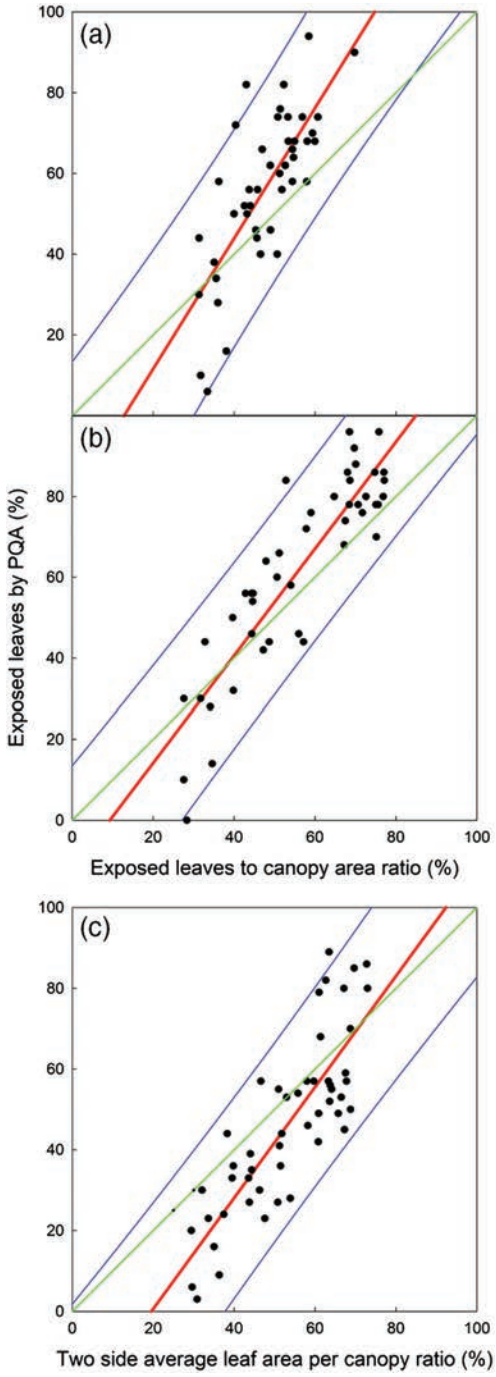


**Figure 8.** Correlations between the leaf to canopy area ratio (%), assessed by image analysis from images acquired using the multi-sensor platform on-the-go and the values determined by point quadrat analysis (PQA), from (a) the east side of the canopy ($R^2$ = 0.57); (b) the west side of the canopy ($R^2$ = 0.79); and (c) the whole vine ($R^2$ = 0.68). All determination coefficients ($R^2$) were significant at $P < 0.001$. Correlation line (——), prediction bands at 95% (——), the 1:1 line (——) ($n$ = 50).

The developed on-the-go imaging system represents an improvement from previous work (Hill et al. 2011, Fernández et al. 2013, Diago et al. 2016) in which robust and reliable image-based methods were developed to quantify grapevine canopy elements. Likewise, in Hill et al. (2011) and Diago et al. (2016) the image-derived outcome was validated against the standard PQA, but a colour background and manual image acquisition were required. Improvements to on-the-go monitoring were recently described by Gatti et al. (2016). These authors acquired RGB images on a stop-and-go mode using a conventional tractor (the tractor driver stopped and triggered the sensor), and obtained a significant correlation between an image-derived canopy index value, which varied between 0 and 1000, and the fraction of canopy gaps and the leaf layer number, as measured by PQA. Another recent approach involved RGB image acquisition on-the-go at low speed, less than 1 km/h, to estimate yield parameters (Rose et al. 2016). In the present study all images were acquired fully automated, on-the-go, without stopping, at a commercial speed of 7 km/h,

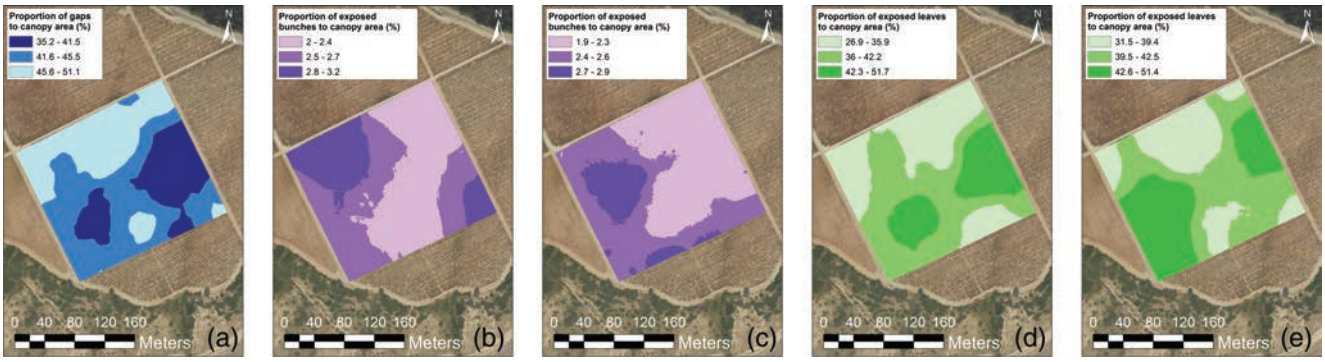


**Figure 9.** Maps of the spatial variability of: (a) canopy porosity or proportion of gaps involving both sides; bunch to canopy area ratio (%) (b) on the east and (c) on the west sides; and leaf to canopy area ratio (%) (d) on the east and (e) on the west sides. Images with the multi-sensor platform were acquired on-the-go at 7 km/h from the east and west sides of the canopy and analysed using the developed methodology.

as the inductive sensor installed in the vehicle triggered the RGB camera at a given frequency as the wheel spins.

Most of the comparisons between the imaging-derived canopy values and those measured by PQA had an $R^2$ close to or above 0.60. Discrepancies between the values obtained by the image method and PQA may be explained by the fact that the accuracy of the PQA method is dependent on the size of the feature to be determined, and the total number of insertions. In terms of the size of the feature in the canopy, the accuracy of PQA was lower for those elements in the image in small proportion, such as the bunches, and in dense canopies, the proportion of gaps or canopy porosity also. To illustrate this, Figure 10 shows two examples of RGB images of vine segments (west side) and the resulting image classification used to build the correlations. In Figure 10a, a small proportion of bunches is visible and exposed, which was quantified as 1.7% by image analysis, while PQA recorded 8%. Similarly, in Figure 10b, the proportion of exposed bunches by image analysis was 5.9% while a 36% value was obtained from PQA. Such differences may arise from the fact that in the PQA method the record of one insertion is extrapolated to an area of 100 $cm^2$ (if insertions are performed on a

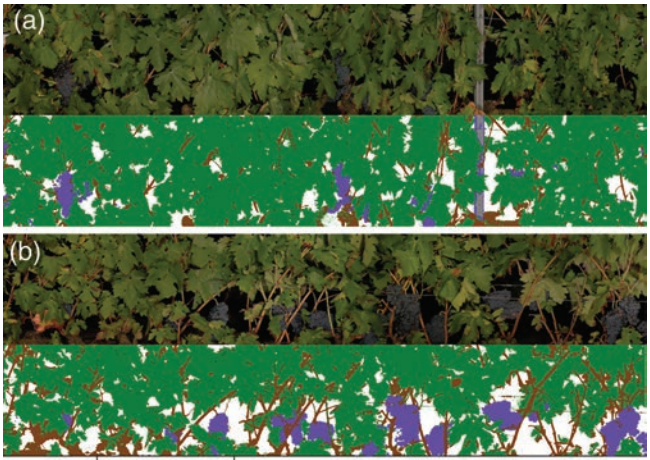


| Segment | Method | Porosity (% gaps) | Exposed leaves to canopy area ratio (%) | Exposed bunches to canopy area ratio (%) |
|---|---|---|---|---|
| a | PQA | 8.0 | 84.0 | 8.0 |
| | Image analysis | 13.3 | 77.1 | 1.7 |
| b | PQA | 20.0 | 44.0 | 36.0 |
| | Image analysis | 18.9 | 57.2 | 5.9 |

**Figure 10.** Comparison of the outputs obtained from point quadrat analysis and image-analysis (table aside) in a canopy segment with (a) low proportion of exposed bunches and (b) medium proportion of exposed bunches.

$10 \times 10$ cm grid, such as in Gatti et al. 2016) to 240 $cm^2$ on average (in the present work). The inconsistencies in the extrapolation of each insertion record are larger for the minority elements, the bunches in Figure 10a,b. The larger the number of insertions, the more accurate are the PQA estimations. This is true up until a given number of insertions (a plateau) is reached. In the image-analysis method, each pixel, with a size of 0.9 $mm^2$/pixel, would correspond to an insertion. In other words, the image-analysis method can be seen as a high-resolution PQA which takes into account the gaps, and only the outer (exposed) layers of the canopy for the visibility of leaves and bunches.

The outcomes of this work may have practical implications for grapegrowers and viticulturists, especially when the results are expressed as georeferenced maps. The ability to adopt different canopy management strategies (such as defoliation or lateral removal on one or both sides) or leaf removal intensity level within a vineyard, according to measured and quantitative values of canopy porosity and leaf and bunch exposure is potentially useful.

In its current version, the image-based methodology can only be applied to red cultivars after veraison. The analysis of white cultivars, or red cultivars before veraison (when berries are still green), is more problematic. While the application of this methodology at early stages (pre-veraison) would increase its adoption in commercial operations, in cool climate regions, bunch thinning and bunch zone leaf removal, are routinely applied separately or in combination at veraison or post-veraison to modify the microclimate in the fruiting zone (Frioni et al. 2017). Changes in the canopy configuration around the bunch zone, especially increased porosity, leading to increased bunch exposure and air circulation, have been shown to positively modify the flavonol profile of berries (Martinez-Lüscher et al. 2019) along with botrytis incidence (Zoecklein et al. 1992, Hed et al. 2015). In addition, bud fruitfulness in cool regions could also benefit from a more exposed, increased light environment of the renewal zones (Dry 2000). Moreover, if leaves have been removed pre-veraison, this image-based methodology may provide a canopy assessment to verify the outcomes of the defoliation operation (either manual or mechanical) in terms of canopy porosity and ratio of exposed leaves and bunches within the bunch microclimate or fruiting zone area. In contrast, if no leaf plucking has been conducted prior to veraison, but is likely to be done later (Frioni et al. 2017), the image-analysis method may provide the initial canopy assessment upon which to adjust the severity of defoliation. Should leaves be removed manually, the

grapegrower may adjust the intensity of, for example, leaf or lateral removal to a desired value of canopy porosity or bunch exposure, to promote air circulation and ensure optimum sunlight capture and temperature. Should defoliation be mechanically conducted, it can also be more precisely accomplished using the new generation of leaf removers, such as those based on leaf blowing in which the pressure of the compressors can be variably adjusted, for instance according to different amounts of exposed leaves.

This image-based methodology, in contrast, can also be adapted to assess not only the fruiting zone, but also the whole canopy above the cordons, with the aim of estimating the 'leaf wall' or leaf coverage prior to spraying applications, at any time during the growing season. Likewise, the built maps could be used by the novel variable rate application machinery to implement more precise and efficient application of, for example, fertiliser and fungicide. Examples of variable dosage of pesticides in different crops based on ultrasound and 3D sensors have been reported (Maghsoudi et al. 2015, Dammer 2016, Tackenberg et al. 2016). In the case of viticulture, the innovation of vineyard machinery with the variable rate technology (Llorens et al. 2010, Gil et al. 2013, Palleja and Landers 2017) relies on automated and accurate assessment of the grapevine canopy growth and development, including an assessment of the canopy porosity and amount of exposed leaves.

Future work will concentrate on adapting the image acquisition process to be undertaken during the day while avoiding the influence of opposite rows. Likewise, the use of much brighter external lights and shorter exposure times can be explored. Nevertheless, the existing system can be mounted on any vineyard vehicle, from a conventional tractor (while conducting mowing or tilling operations), an ATV to even a robot for vineyard monitoring (Rose et al. 2016, Tardaguila et al. 2016).

## Conclusions

In modern viticulture, vineyard management decisions relating to leaf defoliation or spraying are made by informed grapegrowers taking into account vineyard variability. With this in mind, a non-destructive, image-based, on-the-go system was developed to provide information of the grapevine canopy parameters, involving gaps, leaves and fruit. These data can be used to adapt and improve the efficiency (at different levels, qualitative, economic and environmental sides) of a range of canopy management operations. The information can be prepared as maps, which can be used to improve vineyard management decisions and facilitate the use of variable rate machinery.

## Acknowledgements

The authors would like to thank Mr Ignacio Barrio and Mrs Marjolaine Chatin for their help during field measurements of PQA and for help with image processing. The authors would also like to thank the Bodegas Puelles winery (Ábalos, La Rioja, Spain) for the use of their vineyards to conduct this study. Dr Maria P. Diago is funded by the Spanish Ministry of Science, Innovation and Universities with a Ramón y Cajal grant RYC-2015-18429. Dr Borja Millan would especially like to acknowledge the research funding FPI grant 536/2014, by the University of La Rioja (Spain). Dr Fernando Palacios would also like to acknowledge the research funding FPI grant 286/2017 by the University of La Rioja, Government of La Rioja (Spain). This work is part of the ReSoLVe project, for which the authors acknowledge the financial support provided by transnational funding bodies, being partners of the FP7 ERA-net project, CORE Organic Plus and the co-fund from the European Commission. This work has received funding from the European Union's Seventh Framework Programme for research, technological development and demonstration under the Innovine project, with grant agreement no. 311775. Finally, the authors would like to thank Juvé & Camps S.A. and Bodegas Martín Códax S.A.U. for their support through the Globalviti project.

## References

Agoston, M.K. (2005) Color. Agoston, M.K., ed. Computer graphics and geometric modeling: implementation and algorithms (Springer: London, England) pp. 294–307.

Austin, C.N., Gove, G.G., Meyers, J.M. and Wilcox, W.F. (2011) Powdery mildew severity as a function of canopy density: associated impacts on sunlight penetration and spray coverage. American Journal of Enology and Viticulture **62**, 23–31.

Chinchor, N. (1992) MUC-4 evaluation metrics. Morgan Kaufmann Publishers, ed. Proceedings of the fourth message understanding conference; 16–18 June 1992; McLean, VA, USA (Association for Computational Linguistics: Stroudsburg, PA, USA) pp. 22–29.

Chopin, J., Laga, H. and Miklavcic, S.J. (2016) A hybrid approach for improving image segmentation: application to phenotyping of wheat eaves. PLoS One **11**(**12**), e0168496.

Chopin, J., Kumar, P. and Miklavcic, S.J. (2018) Land-based crop phenotyping by image analysis: consistent canopy characterization from inconsistent field illumination. Plant Methods **14**, 39.

Coombe, B.G. (1995) Growth stages of the grapevine: adoption of a system for identifying grapevine growth stages. Australian Journal of Grape and Wine Research **1**, 104–110.

Dammer, K.H. (2016) Real-time variable-rate herbicide application for weed control in carrots. Weed Research **56**, 237–246.

Diago, M.P., Vilanova, M. and Tardaguila, J. (2010) Effects of timing of manual and mechanical early defoliation on the aroma of *Vitis vinifera* (L.) Tempranillo wine. American Journal of Enology and Viticulture **61**, 382–391.

Diago, M.P., Ayestarán, B., Guadalupe, Z., Poni, S. and Tardaguila, J. (2012a) Impact of pre-bloom and fruit-set basal leaf removal on the flavonol and anthocyanin composition of Tempranillo grapes. American Journal of Enology and Viticulture **63**, 367–376.

Diago, M.P., Krasnow, M., Bubola, M., Millán, B. and Tardaguila, J. (2016) Assessment of vineyard canopy porosity using machine vision. American Journal of Enology and Viticulture **67**, 229–238.

Diago, M.P., Correa, C., Millán, B., Barreiro, P., Valero, C. and Tardaguila, J. (2012b) Grapevine's yield and leaf area estimation using supervised classification methodology on RGB images taken under field conditions. Sensors **12**, 16988–17006.

Dokoozlian, N.K. (2009) Integrated canopy management: a twenty-year evolution in California. Dokoozlian, N.K. and Wolpert, J., eds. Recent advances in grapevine canopy management; 16 July 2009; Davis, CA, USA (University of California: Davis, CA, USA) pp. 43–52.

Dry, P.R. (2000) Canopy management for fruitfulness. Australian Journal of Grape and Wine Research **6**, 109–115.

Dunn, G.M. and Martin, S.R. (2004) Yield prediction from digital image analysis: a technique with potential for vineyard assessments prior to harvest. Australian Journal of Grape and Wine Research **10**, 196–198.

Fernández, R., Montes, H., Salina, C., Sarria, J. and Armada, M. (2013) Combination of RGB and multispectral imagery for discrimination of Cabernet Sauvignon grapevine elements. Sensors **13**, 7838–7859.

Frioni, T., Zhuang, S., Palliotti, A., Sivilotti, P., Falchi, R. and Sabbatini, P. (2017) Leaf removal and cluster thinning efficiencies are highly modulated by environmental conditions in cool climate viticulture. American Journal of Enology and Viticulture **68**, 325–335.

Gatti, M., Garavani, A., Vercesi, A. and Poni, S. (2017) Ground-truthing of remotely sensed within-field variability in a cv. Barbera plot for improving vineyard management. Australian Journal of Grape and Wine Research **23**, 399–408.

Gatti, M., Dosso, P., Maurino, M., Merli, M.C., Benizzoni, F., Pirez, F.J., Platè, B., Bertuzzi, G. and Poni, S. (2016) MECS-VINE®: a new proximal sensor for segmented mapping of vigor and yield parameters on vineyard rows. Sensors **16**, 2009.

Gil, E., Llorens, J., Llop, J., Fàbregas, X., Escolà, A. and Rosell-Polo, J.R. (2013) Variable rate sprayer. Part 2: Vineyard prototype: design, implementation and validation. Computers and Electronics in Agriculture **95**, 136–150.

Hed, B., Ngugi, H.K. and Travis, J.W. (2015) Short- and long-term effects of leaf removal and gibberellin on Chardonnay grapes in the Lake Erie region of Pennsylvania. American Journal of Enology and Viticulture **66**, 22–29.

Herrera, F., Charte, F., Rivera, A.J. and del Jesus, M.J. (2016) Multilabel classification. Problem analysis, metrics and techniques (Springer International Publishing: Basel, Switzerland).

Hill, G.N., Beresford, R.M., Wood, P.N., Kim, K.S. and Wright, P.J. (2011) Image-assisted gap estimation, a simple method for measuring grapevine leaf canopy density. Crop Science **51**, 2801–2808.

Jenks, G.F. (1967) The data model concept in statistical mapping. Konrad, F. and Philip, G., eds. International year book of cartography, Vol. **7** (C. Bertelsmann: Gütersloh, Germany) pp. 186–190.

Kliewer, W.M. (1977) Effect of high temperatures during the bloom-set period on fruit-set, ovule fertility, and berry growth of several grape cultivars. American Journal of Enology and Viticulture **4**, 215–222.

Kliewer, W.M. and Dokoozlian, N.K. (2005) Leaf area/crop weight ratios of grapevines: influence on fruit composition and wine quality. American Journal of Enology and Viticulture **56**, 170–181.

Kohavi, R. and Provost, F. (1998) Glossary of terms. Machine Learning **30**, 271–274.

Liu, S., Cossell, S., Tang, J., Dunn, G. and Whitty, M. (2017) A computer vision system for early stage grape yield estimation based on shoot detection. Computers and Electronics in Agriculture **137**, 88–101.

Llorens, J., Gil, E., Llop, J. and Escolà, A. (2010) Variable rate dosing in precision viticulture: use of electronic devices to improve application efficiency. Crop Protection **29**, 239–248.

Maghsoudi, H., Minaei, S., Ghobadian, B. and Masoudi, H. (2015) Ultrasonic sensing of pistachio canopy for low-volume precision spraying. Computers and Electronics in Agriculture **112**, 149–160.

Mahalanobis, P.C. (1936) On the generalised distance in statistics. Proceedings of the National Institute of Sciences of India **12**, 49–55.

Main, G.L. and Morris, J.R. (2004) Leaf-removal effects on *Cynthiana* yield, juice composition, and wine composition. American Journal of Enology and Viticulture **55**, 147–152.

Maktabdar Oghaz, M., Maarof, M.A., Zainal, A., Rohani, M.F. and Yaghoubyan, S.H. (2015) A hybrid colour space for skin detection using genetic algorithm heuristic search and principal component analysis technique. PLoS One **10**(**8**), e0134828.

Martin-Clouaire, R., Rellier, J.P., Paré, N., Voltz, M. and Biarnès, A. (2016) Modelling management practices in viticulture while considering resource limitations: the divine model. PLoS One **11**(**3**), e0151952.

Martinez-Lüscher, J., Brillante, L. and Kurtural, S.K. (2019) Flavonol profile is a reliable indicator to assess canopy architecture and the exposure of red wine grapes to solar radiation. Frontiers in Plant Science **10**, Article 10.

Matthews, B. (1975) Comparison of the predicted and observed secondary structure of T4 phage lysozyme. Biochimica et Biophysica Acta **405**, 442–451.

Mori, K., Goto-Yamamoto, N., Hashizume, K. and Kitayama, M. (2007) Effect of high temperature on anthocyanin composition and transcription of flavonoid hydroxylase genes in 'Pinot noir' grapes (*Vitis vinifera*). Journal of Horticultural Science and Biotechnology **82**, 199–206.

Nuske, S.T., Wilshusen, S.K., Achar, S., Yoder, L., Narasimhan, S.G. and Singh, S. (2014) Automated visual yield estimation in vineyards. Journal of Field Robotics **31**, 837–860.

Palleja, T. and Landers, A.J. (2017) Real time canopy density validation using ultrasonic envelope signals and point quadrat analysis. Computers and Electronics in Agriculture **134**, 43–50.

Palliotti, A. and Silvestroni, O. (2004) Ecofisiologia applicate alla vite. Cozzolino, E., ed. Viticoltura ed enologia biologica (Edagricole: Bologna, Italy) pp. 41–88.

Powers, D.M.W. (2011) Evaluation: from precision, recall and F-measure to ROC, informedness, markedness & correlation. Journal of Machine Learning Technologies **2**, 37–63.

Reynolds, A.G. and Wardle, D.A. (1989) Influence of fruit microclimate on monoterpene levels of Gewürztraminer. American Journal of Enology and Viticulture **40**, 149–154.

Rose, J.C., Kicherer, A., Wieland, M., Klingbeil, L., Töpfer, R. and Kuhlmann, H. (2016) Towards automated large-scale 3D phenotyping of vineyards under field conditions. Sensors **16**, 2136.

Smart, R.E. (1987) Influence of light on composition and quality of grapes. Acta Horticulturae **206**, 37–47.

Smart, R.E. (1992) Canopy management. Coombe, B.G. and Dry, P. R., eds. Viticulture. Volume 2 – Practices (Winetitles: Adelaide, SA, Australia) pp. 85–103.

Smart, R.E. and Robinson, M. (1991) Sunlight into the wine. A handbook for winegrape canopy management (Winetitles: Adelaide, SA, Australia).

Soille, P. (2004) Morphological image analysis – principles and applications, 2d ed. (Springer-Verlag: Berlin, Germany).

Subban, R. and Mishra, R. (2013) Combining color spaces for human skin detection in color images using skin cluster classifier. Singh, A. and Das, V.V., eds. Proceedings of the 5th international conference on advances in recent technologies in electrical and electronics; 20–21 September 2013; Bangalore, India (Lecture Series in Computer Science Volume 5) (International Technology Innovation: Ottawa, ON, Canada) pp. 68–73.

Tackenberg, M., Volkmar, C. and Dammer, K.H. (2016) Sensor-based variable-rate fungicide application in winter wheat. Pest Management Science **72**, 1888–1896.

Tagarakis, A., Liakos, V., Chatzinikos, T., Koundouras, S., Fountas, S. and Gemtos, T. (2013) Using laser scanner to map pruning wood in vineyards. Precision Agriculture **13**, 633–639.

Tardaguila, J., Blanco, J.A., Poni, S. and Diago, M.P. (2012) Mechanical yield regulation in winegrapes: comparison of early defoliation and crop thinning. Australian Journal of Grape and Wine Research **18**, 344–352.

Tardaguila, J., Martinez De Toda, F., Poni, S. and Diago, M.P. (2010) Impact of early leaf removal on yield and fruit and wine composition of *Vitis vinifera* L. Graciano and Carignan. Effects of timing of manual and mechanical early defoliation on the aroma of *Vitis vinifera* (L.) Tempranillo wine. American Journal of Enology and Viticulture **61**, 372–381.

Tardaguila, J., Rovira-Más, F., Blasco, J., Saiz-Rubio, V., Faenzi, E., Évain, S., Labails, S., Stoll, M., Scheidweiler, M., Millot, C. and Campos, E. (2016) VineRobot: a new robot for vineyard monitoring using non-invasive sensing technologies. Proceedings of the ninth international cool climate wine symposium; 26–28 May 2016; Brighton, England. p. 71.

Vandenbroucke, N., Macaire, L. and Postaire, J.G. (1998) Color pixels classification in a hybrid color space. Proceedings of the international conference of image processing (ICIP); 4–7 October 1998; Chicago, IL, USA (Institute of Electrical and Electronics Engineers Computer Society: Washington, DC, USA) p. 176.

Zoecklein, B.W., Wolf, T.K., Duncan, N.W., Judge, J.M. and Cook, M.K. (1992) Effects of fruit zone leaf removal on yield, fruit composition, and fruit rot incidence of Chardonnay and White Riesling (*Vitis vinifera* L.) grapes. American Journal of Enology and Viticulture **43**, 139–148.

*Manuscript received:* 12 December 2018
*Revised manuscript received:* 3 April 2019
*Accepted:* 4 April 2019